Prion Propagation is Dependent on Key Amino Acids in Charge Cluster 2 within the Prion Protein

Savroop Bhamra [†] **Parineeta Arora** [†] **Szymon W. Manka, Christian Schmidt, Craig Brown, Melissa L. D. Rayner, Peter-Christian Klöhn, Anthony R. Clarke** [‡] **John Collinge** [§] **and Parmjit S. Jat** [*§]

MRC Prion Unit at UCL, *UCL Institute of Prion Diseases, Courtauld Building, 33 Cleveland Street, London W1W 7FF, UK*

Correspondence to Parmjit S. Jat: *p.jat@prion.ucl.ac.uk (P.S. Jat)*
https://doi.org/10.1016/j.jmb.2022.167925
Edited by Louise C. Serpell

Abstract

To dissect the N-terminal residues within the cellular prion protein (PrP^C) that are critical for efficient prion propagation, we generated a library of point, double, or triple alanine replacements within residues 23–111 of PrP, stably expressed them in cells silenced for endogenous mouse PrP^C and challenged the reconstituted cells with four common but biologically diverse mouse prion strains. Amino acids (aa) 105–111 of Charge Cluster 2 (CC2), which is disordered in PrP^C, were found to be required for propagation of all four prion strains; other residues had no effect or exhibited strain-specific effects. Replacements in CC2, including aa105-111, dominantly inhibited prion propagation in the presence of endogenous wild type PrP^C whilst other changes were not inhibitory. Single alanine replacements within aa105-111 identified leucine 108 and valine 111 or the cluster of lysine 105, threonine 106 and asparagine 107 as critical for prion propagation. These residues mediate specific ordering of unstructured CC2 into β-sheets in the infectious prion fibrils from Rocky Mountain Laboratory (RML) and ME7 mouse prion strains.

Introduction

Prion diseases are fatal progressive neurodegenerative maladies that involve accumulation of assemblies of an aberrantly folded PrP^C. Misfolding of PrP^C is an autocatalytic process of seeded fibrillization and fission and involves dramatic changes to the conformation of PrP, from an α-helix-rich to a β-sheet-rich protein.[1–4] Recent electron microscopic analyses of high-titre exceptionally pure infectious prions have identified rods comprised of single-protofilament helical amyloid fibrils[5–6] and twisted pairs of the same protofilaments[6–9]; each rung of the protofilament is a single PrP monomer.

PrP^C is a highly conserved cell-surface glycoprotein, expressed in most cell types, but without a precise unitary cellular function, although many roles have been proposed.[10–12] The wide variety of activities and functions ascribed to PrP^C suggest that it does not act exclusively in a single pathway, but may function as a dynamic scaffold for the assembly of various multicomponent signalling complexes while it moves between the cell surface and the endocytic compartment.[10–12] PrP^C undergoes misfolding after coming into contact with prions primarily at the cell surface[13], with the newly formed prions residing attached to the cell membrane.[14]

Mice devoid of PrP ($Prnp^{0/0}$) are viable, have no overt phenotype but are completely resistant to prion disease indicating that PrP is essential for pathogenesis.[15–18] Development of these $Prnp^{0/0}$ mice led to an extensive structure–function analysis

of PrP to identify domains that are important for prion propagation by reconstituting these mice with mutant PrP transgenes. This demonstrated that N-terminally truncated PrP (Δ23-80, Δ32-80 and Δ32-93) could be converted to infectious prions but at a reduced level of susceptibility,[18–19] whereas PrP Δ32-106 could not be converted to disease-associated PrP nor supported RML prion propagation upon reconstitution of *Prnp*$^{0/0}$ mice.[20] This was further supported by Suppatapone *et al* who found that reconstitution of *Prnp*$^{0/0}$ mice with PrP Δ23-88 propagated prions but with a longer incubation time.[21]

The N-terminal half of PrP^{C} is glycine-rich and disordered. It encompasses two charge clusters, denoted CC1 (polybasic region, 23.KKRPK.27) and CC2 (90.QGGGTHNQWNKPSKPKTNLKHV.111), octapeptide repeats (OPRs, 51–90), and an alanine-rich low-complexity region (LCR, 112.AGAAAAGAVVGGLGG.126). The CC1 domain is fundamental for: (i) PrP^{C} endocytosis via coated pits[22]; (ii) overall folding of the globular C-terminal domain[23]; (iii) efficiency of prion propagation in transgenic mice.[24] The octapeptide repeat region (OPR, 51–90), contains one cryptic and four consensus repeats of eight amino acids. Supernumerary insertions of between one and nine additional OPRs may increase the risk of developing disease with most cases showing an earlier onset[25]. Deletion mutagenesis studies have suggested that the OPRs are not required for prion propagation, and play only a limited role in disease pathogenesis.[26] The function of OPRs remains unclear but they can bind divalent metal ions through coordination to histidine residues and may play a role in copper homeostasis.[27] CC2 is one of the most immunogenic regions of PrP^{C} and reported to be the interaction site for amyloid-beta oligomers[28–32], heparin and copper.[33] It is also proposed to specifically bind disease-associated PrP, leading to seeded misfolding of PrP^{C}[34]. CC2 also contains the highly conserved central lysine cluster (CLC) of four lysines surrounding the prolines at residues 101 and 104. Substitution of these lysines with alanine or asparagine enhanced the formation of more pathogenic synthetic aggregates upon prion-templated seeding in the absence of co-factors[35]. The two prolines are mutated in human Gerstmann-Straussler-Scheinker syndrome, giving rise to a distinctly different prion fibril structure[36], compared to all rodent prion fibril structures determined to date[5–6,9,37–38]. P102L mutation promotes prion-seeded amplification without co-factors and spontaneous prion formation in combination with mutation of the four lysines.[39]

In addition to reconstitution of *Prnp*$^{0/0}$ mice, many of these mutant transgenes were also used to study prion propagation *in vitro* in cells expressing endogenous PrP^{C}, or chronically prion-infected N2a (ScN2a) cells.[34,40–42] However these results may have been compromised by the presence of endogenous PrP as Supattapone *et al.* observed that upon RML infection, mouse wild-type PrP (moPrP^{WT}) can act in *trans* to accelerate propagation of a PrP double deletion mutant (Δ23-88 and Δ141-176) in transgenic mice.[43] There is a further complication in that many previous studies have used the 3F4 epitope to distinguish the exogenously introduced protein from the endogenous protein. The epitope for the 3F4 antibody is generated by mutating leucine 108 and valine 111 to methionine in mouse PrP. They found that the presence of the 3F4 epitope in PrP has a non-strain specific adverse effect on prion propagation in transgenic mice.[21]

Just as the development of *Prnp*$^{0/0}$ mice paved the way for a structure–function analysis of PrP in mice by transgenic expression of N-terminal deletion mutants[15,18]; our aim was to identify which residues within the unstructured amino-terminal domain were required for prion propagation in cells. We did this by: (i) generating cells stably knocked-down for PrP^{C} expression to a level that renders them fully resistant to prion infection, while regaining susceptibility to infection upon restoring PrP expression; (ii) preparing a library of single, double and triple replacements of all residues, except proline and glycine, to alanine within the N-terminal 23–111 region and assaying their ability to support propagation of RML prions. We extended our study to three other prion strains, ME7, 22L and MRC2 in CAD5 cells. Like RML, 22L and ME7 are mouse-adapted scrapie prion strains with a relatively short incubation period, whereas MRC2 is a mouse-adapted bovine spongiform encephalopathy (BSE) prion strain characterised by a long incubation time and di-glycosylation-dominant PrP^{Sc}[44] and may represent the same strain as 301C.[45] The rationale for this mutagenesis approach was informed by extensive research showing that elimination of side-chains beyond the β-carbon by alanine replacement, with minimal perturbation of the protein backbone conformation, can probe the influence of specific amino acid side-chains on biological activity, protein stability or folding.[46–47] It is applicable to a wide range of amino acids, as it contains an inert, non-bulky methyl group, and retains the secondary structure preferences of many amino acids, thus minimally affecting secondary structure.[47–48] Proline and glycine residues were not targetted for mutagenesis in this study to minimise the amount of structural change as they provide rigidity and flexibility respectively, to the protein backbone.

Results

PK1-KD cells: A stable cell line knocked-down for expression of endogenous prion protein

To study the effect of *Prnp* mutations on prion propagation without interference from endogenous PrP^{C}, we stably silenced it in PK1-10 cells, a cell

line highly susceptible to RML infection, using the pRetroSuper vector system. PK1-10, are a single cell clone of the PK1 cells which is a clone of mouse N2a neuroblastoma cells that are highly susceptible to prion infection and able to maintain a chronic RML prion infection.[49] PK1-10 cells are referred to as PK1 from hereon as the only sub-clone of PK1 cells used in this study.

Eight different hairpins, predominantly targetting the 3′ untranslated region (UTR) of endogenous PrP^{C} (Figure 1(A)), were stably expressed in PK1 cells. Bulk cultures of stably transduced cells were prepared and western blotted to determine PrP^{C} expression; shRNA8 markedly reduced PrP expression. Retrovirus encoding shRNA8 was used to repeat transduction of PK1 cells and isolate single cell clones. 96 clones were isolated, reconstituted with the full-length open reading frame (ORF) for $moPrP^{WT}$ (pLNCX2$moPrP^{WT}$) and challenged with RML prions in a scrapie cell assay (SCA), a highly sensitive quantitative cell-based infectivity assay.[49] In SCA, a pre-determined number of cultured cells are infected with prions and serially passaged for three splits to dilute out the original innoculum. At the 4th, 5th and 6th splits, the number of cells containing PK-resistant PrP (PrP^{Sc}) is assessed via ELISPOT using the anti-PrP antibody, ICSM18. Cells containing PK-resistant PrP at this stage represent stably infected cells propagating prions. The relationship between number of infected cells and infectivity as measured in Tissue culture infectious units (TCIU) is not linear (detailed in Figure S1). Split 6 data is presented within the body of the paper while complete data sets (4th, 5th and 6th splits) are provided as supplementary data.

Three clones isolated from PK1shRNA8 bulk culture (9, 43 and 46) that did not propagate prions but regained full susceptibility to RML upon reconstitution with $moPrP^{WT}$, indicated by increasing numbers of PrP^{Sc}-containing cells upon passaging, were identified. PK1shRNA8 clone 9 was one such clone (Figure 1(B and C)); it has been designated PK1-KD and was used for the reconstitution experiments. Compared with non-silenced cells, the level of endogenous PrP in PK1-KD cells was reduced by 88% (Figure 1(D)). PK1-KD cells are resistant to RML infection (Figure 1(E)), but when reconstituted with $moPrP^{WT}$ regain full susceptibility to infection (Figure 1(F)).

Propagation of RML prions is modulated by three distinct domains in the N-terminus of PrP

Suppatapone *et al* found that N-terminal amino acids 23–88 (Figure 2(A)) were required in transgenic mice for efficient prion propagation. To determine if this would be replicated in cultured cells, we reconstituted PK1-KD cells with moPrP Δ23-88, analysed the resulting bulk cultures for cell surface PrP expression (Figure2(B)) and challenged them with RML prions (Figure 2(C) and Figure S2(A)). The effect of Δ23-88 was stronger in PK-1KD cells than in $Prnp^{0/0}$ mice, as it completely abrogated prion propagation. To determine which specific N-terminal residues were critical for prion propagation, single, double and triple replacements to alanine were prepared (Figure 3(A)), used to reconstitute PK1-KD cells and the bulk cultures challenged with RML (Figure 3(B, C & E), Tables S1-3 in Figure S9 and Figure S2(B, C & E)). Two sites, residues 23–25 (KKR), within CC1 domain and glutamine 41 were found to be required. Mutants K23A.K24A.R25A (KKR) and Q41A exhibited considerably reduced RML propagation (Figure 3(B), Table S1 in Figure S9 and Figure S2(B)). While cells that fully supported prion propagation consistently reported over 800 PrP^{Sc} containing cells (number of

Figure 1. PK1-KD cells. (A). Eight siRNA constructs were designed against the native mouse PrP sequence and used to develop shRNA constructs for stable silencing of expression. Of these, shRNA8 was used to establish cells knocked-down for mouse PrP expression. (B). Western blot showing PrP detected in PK1 cells; loss of PrP expression was observed in the bulk culture where shRNA8 was used for silencing. Higher level of suppression of PrP expression was observed in clones 9, 43 and 46. Clone 9 was selected for this study. (C). Immunofluorescence data showing PrP expression in PK1 and PK1-KD cells respectively. DAPI, nuclear stain; mouse PrP, green. (D). Quantification of protein expression by dot blot showed that the level of PrP silencing achieved in PK1-KD cells was 88%. *P-values* were calculated using an unpaired t-test; *** denotes $p \leq 0.0001$, ** $p \leq 0.0005$ and * $p \leq 0.005$. (E). Images of individual ELISPOT wells showing one with typically high spot numbers for PK1 cells infected with RML (1000 spots) and low spot numbers for both RML infected PK1-KD cells and non-infected (NI) PK1 cells (23 and 10 spots respectively). Positive (green) and negative (red) spots are highlighted by the imaging software over a purple background from colour development in the ELISPOT procedure. F. SCA data showing number of infected cells detected upon infection with RML [10^{-5} dilution of 10% infected brain homogenate (BH)]. PK1 cells and PK1-KD cells reconstituted with $moPrP^{WT}$ report full susceptibility to infection (>500 spots), while PK1-KD cells and those transduced with the empty vector, pLNCX2, were resistant to RML infection (<50 spots). Significance was calculated in a one-way ANOVA with Bonferroni correction for multiple comparisons to PK1-KD cells reconstituted with $moPrP^{WT}$. It is indicated by *** for $p \leq 0.0001$. (For interpretation of the references to colour in this figure legend, the reader is referred to the web version of this article.)

A

siRNA	Target sequence (sense)	base pair
1	AACCAACCTCAAGCATGTGGC	499-519
2	AATGTACAGTAGACCAGTTGC	1101-1121
3	AACGATAGCTGATTGAAGGCA	1421-1441
4	AATCTGCATGTACTTCACGTT	2068-2088
5	GAGAGACAATCTAAACATT	1722-1740
6	TAGGAGATCTTGACTCTGA	1541-1559
7	GAAATTCTGCTAGCATTGT	1789-1807
8	GAGACAATCTAAACATTCT	1724-1742

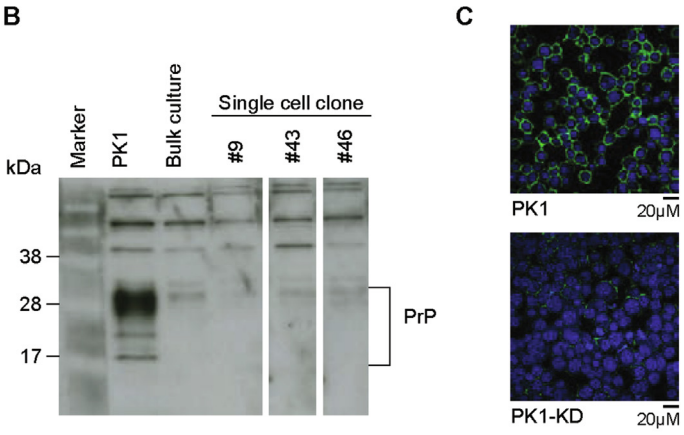

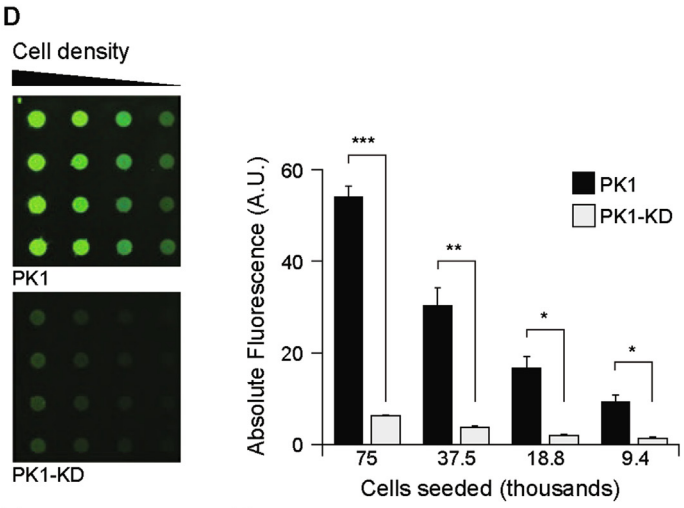

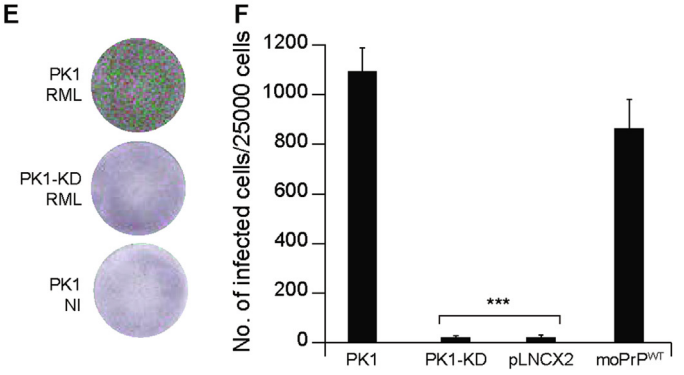

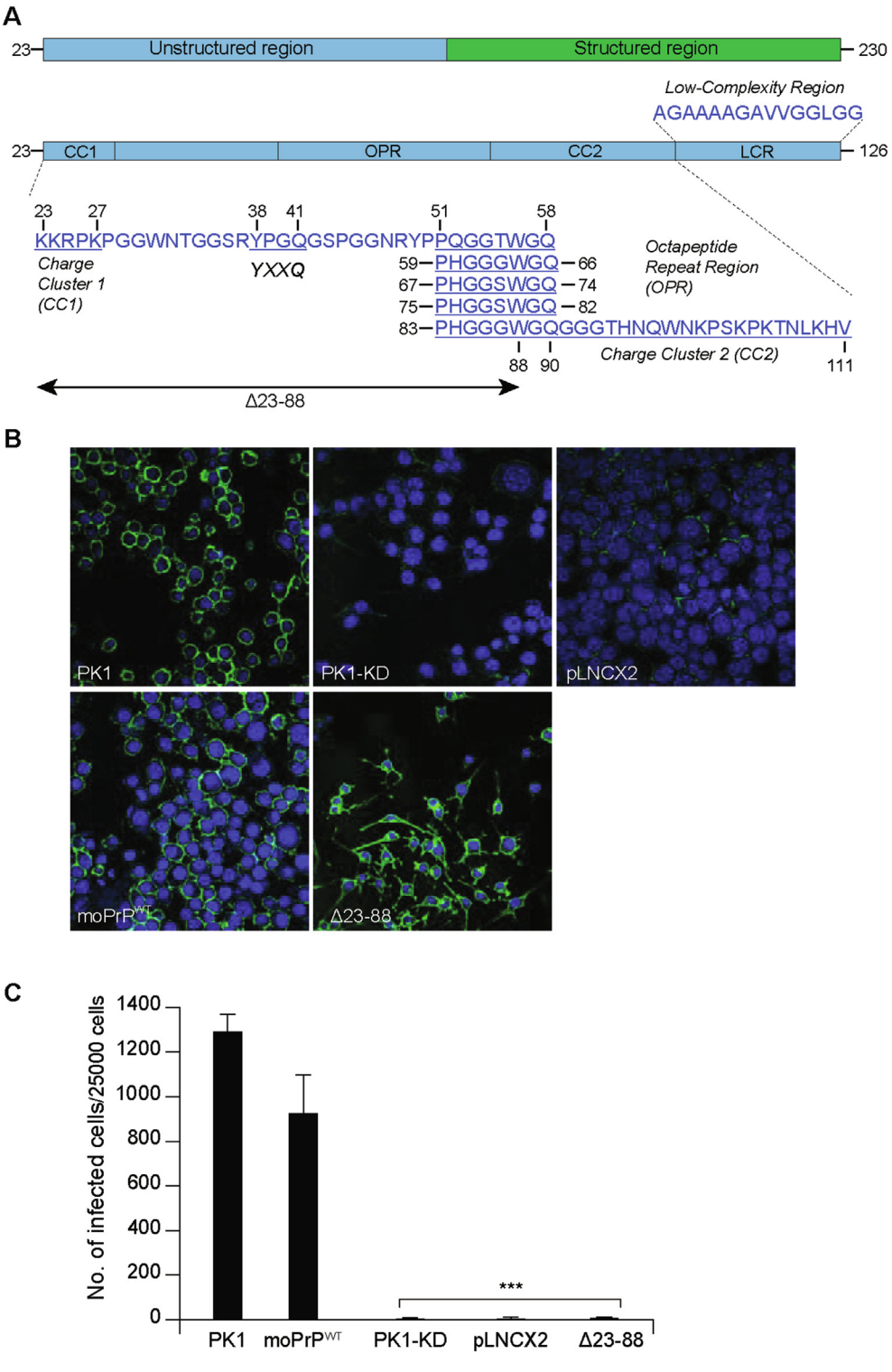
A
23
Unstructured region
Structured region
230
Low-Complexity Region
AGAAAAGAVVGGLGG
23
CC1
OPR
CC2
LCR
126
23 27 38 41 51 58
KKRPKPGGWNTGGSRYPGQGSPGGNRYPPQGGTWGQ
Charge Cluster 1 (CC1)
YXXQ
59 PHGGGWGQ 66
67 PHGGSWGQ 74
75 PHGGSWGQ 82
83 PHGGGWGQGGGTHNQWNKPSKPKTNLKHV
Octapeptide Repeat Region (OPR)
88 90
Charge Cluster 2 (CC2)
111
Δ23-88
B
PK1
PK1-KD
pLNCX2
moPrP^WT
Δ23-88
C
No. of infected cells/25000 cells
1400
1200
1000
800
600
400
200
0
***
PK1
moPrP^WT
PK1-KD
pLNCX2
Δ23-88

infected cells), less than 200 were observed for both KKR and Q41A mutants. This number is much lower than PK1 and PK1-KDmoPrP^{WT} (moPrP^{WT}) cells, yet greater than PK1-KD and PK1-KDΔ23-88 cells (which do not propagate RML prions) suggesting that prion propagation is markedly compromised, but not abrogated.

Rather unexpectedly, no mutation within the OPRs (51–90) was found to reduce prion propagation (Figure 3(B & C), Table S1 & 2 in Figure S9, Figure S2(B & C)). Alanine mutations tested encompassed all OPRs and also included point mutations Q52A, Q58A, H60A, W64A, Q66A, H68A, Q74A, H76A, Q82A, H84A and W88A, and double mutations T55A.W56A, S71A.W72A and S79A.W80A. PK1-KD cells reconstituted with S43A, the triple mutant N47A.R48A.W49A and the OPR mutants yielded number of infected cells $\geq$ PK1 and moPrP^{WT} cells (Figure 3(B), Table S1 in Figure S9 and Figure S2(B)).

To investigate whether reduced prion propagation in the KKR (23–25) mutant was due to removal of the three charged residues, or mutation of one key residue, single replacements K23A, K24A and R25A were prepared. When assayed for prion propagation, none of the cells expressing single replacements displayed reduced number of infected cells compared to moPrP^{WT} (Figure 3(D), Table S3 in Figure S9 and Figure S2(D)). To determine if KKR (23–25) was the critical domain, or neighbouring residues also contributed, cells expressing mutations P26A.K27A, P28A and W31A.N32A.T33A were generated and challenged with RML prions. None of them reduced prion propagation relative to moPrP^{WT}, delineating KKR (23–25) as the modulator of prion propagation (Figure 3(D) and Figure S2(D)). When mutation of KKR was combined with mutation of Q41, the effects on RML propagation were not exacerbated (Figure 3(D), Tables S3 in Figure S9 and Figure S2(D)). Since mutation of KKR or Q41 or a combination thereof (K23A.K24A.R25A.Q41A) was not as inhibitory as Δ23-88, it suggested that either all the other residues within the 23–88 region contribute slightly, or the Δ23-88 deletion perturbs the native folding of PrP,[23] thereby reducing its availability as a substrate for prion propagation.

Next we investigated the adjacent aa90-111 CC2 domain's effect on prion propagation. Remarkably, all mutations within the CC2 region, demarcated by Q90A and H110A.V111A (Figure 3(A)), markedly reduced RML propagation. They produced significantly fewer infected cells compared to moPrP^{WT} and PK1 cells. Infected cell numbers for CC2 mutations were above background (PK1-KD and Δ23-88), comparable to Q41 but less than the KKR mutant (Figure 3(B), Table S1 in Figure S9 and Figure S2(B)). To determine if increasing the available pool of infectious prions would improve the propagation profile of PK1-KD cells reconstituted with mutations at KKR, Q41 and within CC2, SCA was conducted with a tenfold higher dose of RML (10^{-4} dilution of 10% infected brain homogenate). Indeed, cells reconstituted with KKR, Q41A and K23A.K24A.R25A.Q41A resulted in higher numbers of infected cells with higher doses of RML innoculum (Figure S3(A)). However, none of the cells expressing CC2 mutants showed significantly increased prion propagation, although a mild increase in infected cells was noted for mutation N99A.K100A (Figure S3(B)). All effects on prion propagation for the reported mutants were verified in three independent clonal cell lines isolated from a repeat reconstitution of PK1-KD cells (Figure 3(E) and Figure S2(E)). Together these results indicated that mutations at aa23-25 (KKR, within CC1), 41 (Q41) and 90–111 (CC2) significantly reduced propagation of RML prions. The reduction was greater for the CC2 mutants than KKR (23–25), or KKRQ (23–25, 41) combined.

Mutations within the CC2 domain dominantly inhibit prion propagation in PK1 cells

PK1 cells were stably transduced with Δ23-88, KKR (23–25) and CC2 mutants and the resulting cells challenged with RML to assess whether these mutations would interfere with prion propagation when co-expressed with wild type PrP^{C}. All six mutations tested within CC2 significantly reduced prion propagation, whereas

Figure 2. N-terminal sites in moPrP targeted for mutagenesis. (A). Schematic showing the full-length mature mouse prion protein (moPrP, aa23-230) with regions of the unstructured amino-terminal domain highlighted as CC1 (Charge Cluster 1), OPR (Octapeptide Repeats), CC2 (Charge Cluster 2) and LCR (Low-Complexity Region). The amino acid sequence is displayed below or above the bars in single letter code with regions of interest highlighted (mouse PrP numbering). (B). Immunofluorescence images showing PrP expression in PK1, PK1-KD and PK1-KD cells reconstituted with empty vector pLNCX2, moPrP^{WT} and mutant Δ23-88. DAPI, nuclear stain; mouse PrP, green. (C). SCA data showing spot numbers for PK1, PK1-KD and reconstituted PK1-KD cells at split 6, post-RML infection [10^{-5} dilution of 10% infected BH]. For SCAs, significance was calculated in a one-way ANOVA with Bonferroni correction for multiple comparisons to PK1-KD cells reconstituted with moPrP^{WT}. It is indicated by *** for $p \leq 0.0001$. (For interpretation of the references to colour in this figure legend, the reader is referred to the web version of this article.)

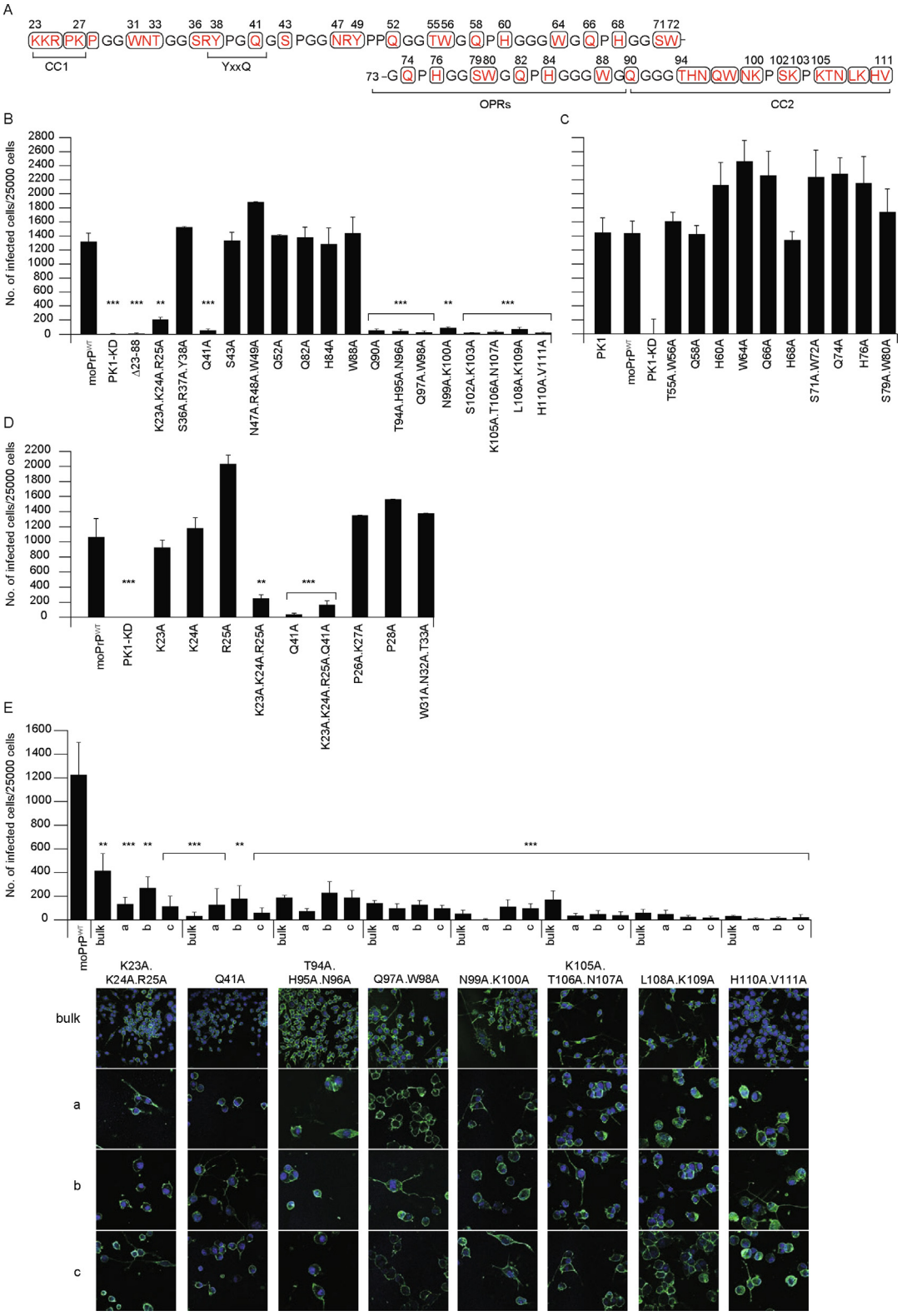
A
CC1
YxxQ
OPRs
CC2
B
No. of infected cells/25000 cells
moPrP^WT
PK1-KD
Δ23-88
K23A.K24A.R25A
S36A.R37A.Y38A
Q41A
S43A
N47A.R48A.W49A
Q52A
Q82A
H84A
W88A
Q90A
T94A.H95A.N96A
Q97A.W98A
N99A.K100A
S102A.K103A
K105A.T106A.N107A
L108A.K109A
H110A.V111A
C
PK1
moPrP^WT
PK1-KD
T55A.W56A
Q58A
H60A
W64A
Q66A
H68A
S71A.W72A
Q74A
H76A
S79A.W80A
D
No. of infected cells/25000 cells
moPrP^WT
PK1-KD
K23A
K24A
R25A
K23A.K24A.R25A
Q41A
K23A.K24A.R25A.Q41A
P26A.K27A
P28A
W31A.N32A.T33A
E
No. of infected cells/25000 cells
moPrP^WT
bulk
a
b
c
K23A. K24A.R25A
Q41A
T94A. H95A.N96A
Q97A.W98A
N99A.K100A
K105A. T106A.N107A
L108A.K109A
H110A.V111A

KKR and Δ23-88 mutations had no effect (Figure 4 (A) and Figure S4). PK1 cells expressing CC2 mutants Q97A.W98A, N99A.K100A, L108A. K109A, and H110.V111A yielded slightly higher numbers of infected cells than Q90A and T94A. H95A.N96A at split 6, though all gave considerably fewer spots than Δ23-88 and KKR cells, which showed no reduction in prion propagation (Figure 4(A) and Figure S4). The lack of prion propagation inhibition by KKR and Δ23-88 mutants in PK1 cells suggests that they suffer bioavailability or folding defects,[23] which prevents them from interfering with prion propagation. In contrast, the CC2 mutants clearly block propagation when co-expressed with wild type PrP^{C}; they may be avidly recruited to prion fibrils and thereby perturb their assembly and/or fission. Our finding that Δ23-88 and mutation of KKR do not inhibit propagation when co-expressed with $moPrP^{WT}$ agrees with previous observations that upon RML infection, $moPrP^{WT}$ can act in *trans* to propagate prions despite the co-expression of a PrP double deletion mutant (Δ23-88 and Δ141–176) in transgenic mice.[21]

Mutation of KKR (23–25), Q41 and the CC2 domain inhibit formation of de novo prions in uninfected cells but do not inhibit an established prion infection

To determine if the KKR, Q41 and CC2 domain mutations would exert a curing effect in cells with an existing prion infection, they were expressed in chronically RML prion-infected PK1 (iPK1) cells. iPK1 cells were stably transduced with retroviruses encoding KKR (23–25), Q41 and four CC2 [QW (97–98), NK (99–100), KTN (105–107) and LK (108–109)] mutants and the resulting cells assessed for levels of PrP^{Sc} by ELISPOT. No marked differences were found in the infected cell numbers between iPK1pLNCX2 (empty vector control) or iPK1 cells transduced with KKR, Q41 or CC2 mutants, indicating that mutations in these regions exerted no control over an established prion infection as their expression in iPK1 cells did not, 'cure' the cells of infection (Figure 4(B)).

Are KKR (23–25), Q41 and the CC2 domain required for propagation of 22L, ME7 and MRC2 prions?

To determine if these three regions were also required for propagation of other common mouse prion strains, CAD-2A2D5 (CAD5) cells, that are susceptible to RML, ME7, 22L and the BSE-derived 301C strain of prions[45,50] were utilised. Endogenous PrP^{C} was silenced using shRNA8, as used for silencing PK1 cells. Bulk cultures of stably transduced cells were negatively sorted for cell surface expression of PrP^{C} by fluorescence-activated cell sorting (Emma Quarterman and Gigi Yang, unpublished work). The sorted cells were single cell cloned; 24 clones were isolated, reconstituted with full-length $moPrP^{WT}$ and challenged with 22L and MRC2 (a mouse-adapted BSE strain)[44] to identify a clone that regains full susceptibility upon reconstitution. This identified clone CAD5-KDB3, that has highly reduced levels of PrP RNA (<1% of the level in CAD5 cells, Figure 5(A)), essentially no detectable cell surface PrP^{C} expression and can propagate 22L, MRC2 and ME7 prions upon reconstitution with $moPrP^{WT}$ (Figure 5(B) & 6(A), Figure S5 & 6). CAD5-KDB3 cells are referred to as CAD5-KD from hereon as the only subclone used for reconstitution.

CAD5-KD cells were stably reconstituted with Δ23-88, KKR, Q41 and CC2 mutants and drug resistant colonies pooled to prepare bulk cultures. Figure 5(C&D) and Figure S6&7 show representative experiments where independently derived bulk cultures for each mutant were challenged in turn with ME7, MRC2 and 22L prions. The results for ME7 (Figure 5(C & D), Tables S4 & 5 in Figure S9 and Figure S6 & 7) were akin to those with RML albeit with two differences. ME7 propagation was unaffected by mutation of Q41, whereas mutation of S43 reduced infected cell numbers, which increased at splits 5 and 6, indicating a lower level of propagation. In contrast, the results for 22L (Figure 5(C & D), Tables S4 & 5 in Figure S9 and Figure S6 & 7) showed that mutation of KKR or Q41 did not affect propagation, as infected cell numbers were similar to $moPrP^{WT}$. Cells

Figure 3. SCA for N-terminal alanine mutations in moPrP (A). All residues other than proline, glycine and existing alanine (black) within the N-terminal 23–111 region were targeted for mutagenesis (red, circled). (B). SCA data for split 6, post-RML infection [10^{-5} dilution of 10% infected BH] of PK1-KD and bulk cultures of PK1-KD cells reconstituted with full length $moPrP^{WT}$ and the indicated moPrP mutants. (C). SCA data for the indicated mutants post-RML infection [10^{-4} dilution of 10% infected BH]. (D). SCA data for mutants within region 23–41 post-RML infection [10^{-5} dilution of 10% infected BH. (E). SCA data post-RML infection [10^{-5} dilution of 10% infected BH and immunofluorescence images of single cell clones of PK1-KD cells after reconstitution with the indicated moPrP mutants showing PrP expression. DAPI, nuclear stain; mouse PrP, green. For SCAs, where number of infected cells was reduced, significance was calculated in a one-way ANOVA with Bonferroni correction for multiple comparisons to PK1-KD cells reconstituted with $moPrP^{WT}$. It is indicated by *** for $p \leq 0.0001$, ** for $p \leq 0.0002$, * for $p \leq 0.005$.[62]

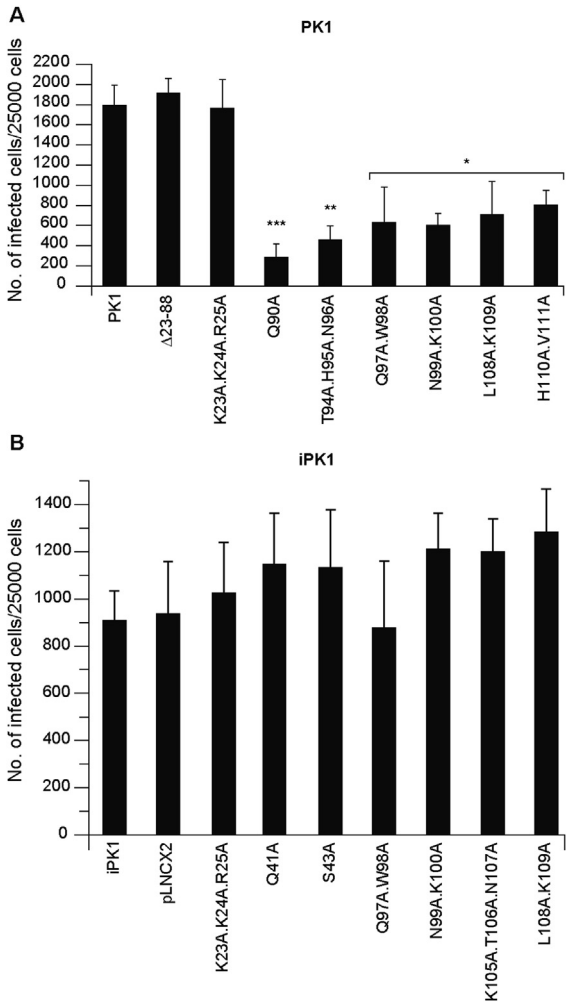

Figure 4. N-terminal residues regulate prion infection. (A). PK1-cells were stably transduced with retrovirus encoding moPrP with alanine mutations and the resultant cells (expressing both endogenous PrP^{C} and mutant moPrP) assayed for their sensitivity to RML prions [10^{-5} dilution of 10% infected brain homogenate] in SCA at split 6. For SCAs, where number of infected cells was reduced, significance was calculated in a one-way ANOVA with Bonferroni correction for multiple comparisons to PK1 cells. It is indicated by *** for $p \leq 0.0001$, ** for $p \leq 0.0002$, * for $p \leq 0.005$.[62] (B). Chronically prion-infected iPK1 cells were stably transduced with retroviruses encoding moPrP alanine mutants and seeded onto ELISPOT plates for detection of PrP^{Sc} positive spots at split 3 post-transduction.

reconstituted with Δ23-88 were slightly reduced in propagation of 22L in comparison to $moPrP^{WT}$, but exhibited an increased number of infected cells at three consecutive splits, indicating propagation of 22L prions. Results for CC2 domain mutants were more surprising. Mutants Q90A, N99A.K100A and S102A.K103A supported propagation of 22L whereas mutants Q97A.W98A, K105A.T106A.N107A, L108A.K109A and H110A.V111A did not. Mutant T94A.H95A.N96A supported a reduced level of propagation of 22L (Figure 5(D), Table S5 in Figure S9 and Figure S7). The MRC2 strain (Figure 5(C & D), Table S4 in Figure S9 and Figure S6) generally produced lower numbers of infected cells than the other three strains. Mutation of Q41 and S43 did not affect propagation whereas Δ23-88 clearly inhibited propagation. The results for CC2 mutants were similar to those with 22L. However, in this case mutants Q97A.W98A, N99A.K100A and S102A.K103A supported MRC2 propagation whereas mutants Q90A, K105A.T106A.N107A, L108A.K109A and H110A.V111A were unable to support propagation. Cells transduced with T94A.H95A.N96A propagated MRC2 even more efficiently than cells reconstituted with $moPrP^{WT}$. Rather surprisingly, CAD5-KD cells reconstituted with mutant Q41 were found to support propagation of RML, whereas this mutant did not support RML propagation in PK1-KD cells (compare Figure 5(D) with Figure 3(B & C)) indicating that glutamine 41 is required for propagation of RML in PK1 cells but not in CAD5 cells.

To identify which amino acids within the 105–111 region were critical for propagation of the four-prion strains, each residue was individually mutated to alanine. Mutant T106A.N107A was also prepared since aa105-107 (KTN) had originally been mutated together. Bulk cultures derived upon reconstitution with these mutants were challenged in turn with RML, ME7, 22L and MRC2 prions simultaneously; a representative SCA is shown in Figure 5(E), Table S6 in Figure S9 and Figure S7. The results showed that mutation of K109 did not affect propagation of any of the four prion strains, whereas mutation of K105 did not affect propagation of RML, MRC2 and 22L; mutation of H110 fully supported propagation of 22L but RML only at a reduced level. In contrast, mutation of L108 and V111 severely impacted propagation of the four prion strains. Mutation of L108 and V111 alone was as effective as mutation of LK (108–109) or HV (110–111) except L108A.K109A was more inhibitory for MRC2 than L108A. Only when K105.T106.N107 were mutated to alanine together, did they impede propagation of the four prion strains.

To confirm that the observed effects on prion propagation were a direct consequence of the mutations, protein expression in CAD5-KD cells expressing these mutants was examined by western blotting and laser-scanning confocal microscopy. The results in Figure 6(A & B) show that although expression was variable, all the mutants were generally expressed at levels higher than endogenous PrP^{C} and predominantly on the cell surface. Moreover, the mutants exhibited the same pattern of three bands corresponding to endogenous PrP^{C} that is non-, mono- and di-

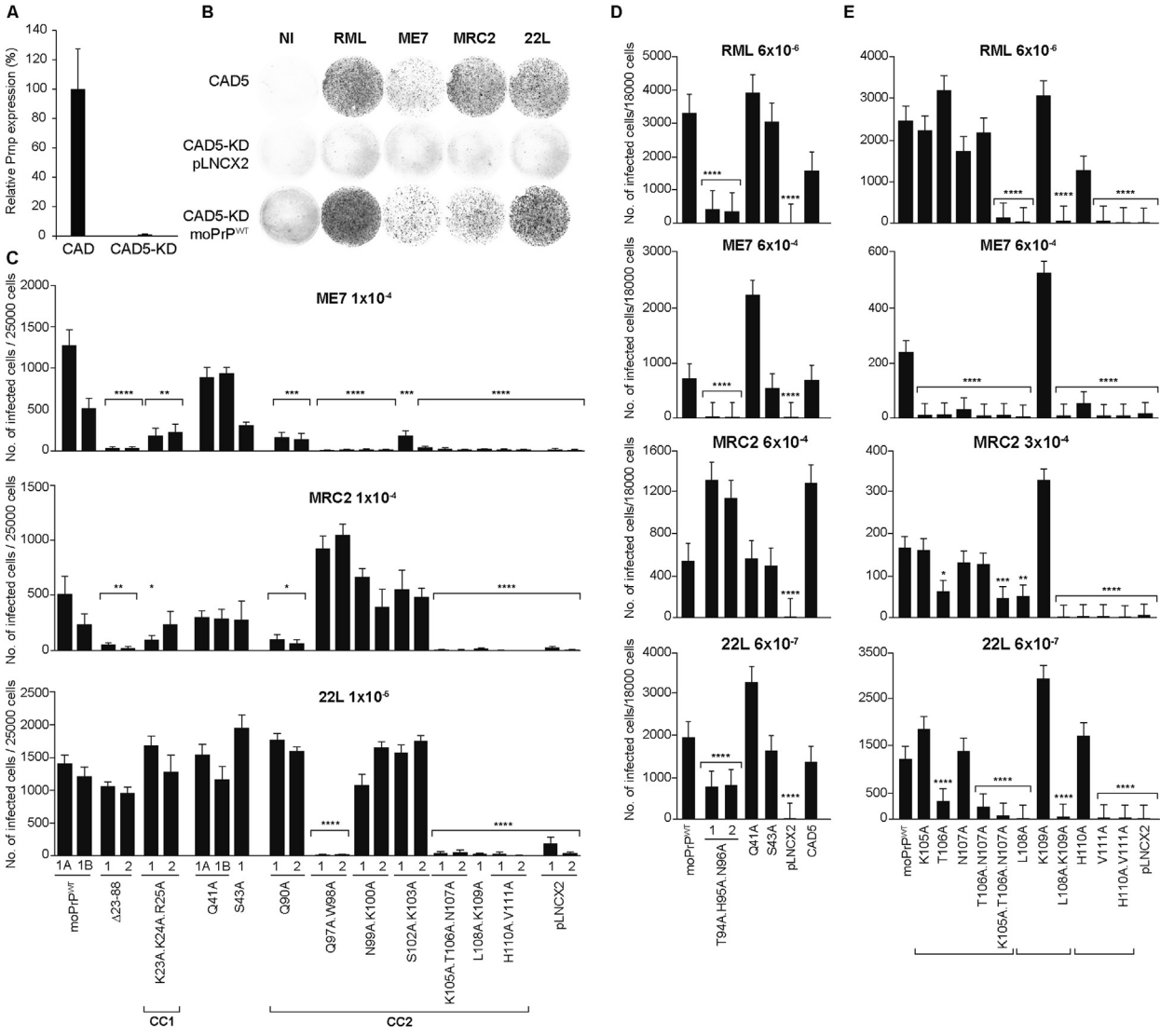

Figure 5. SCA for N-terminal alanine mutations in CAD5-KD cells (A). Expression of *Prnp* in CAD5-KD cells was measured relative to CAD5 cells by RT-PCR. The reactions were carried out in triplicate; the error bars show the standard deviation. *Prnp* expression in CAD5-KD cells was found to be reduced to <1% of the expression in CAD5 cells. (B). Representative images of individual ELISPOT wells at split 6 taken from the expt. presented in (D). They show CAD5 and CAD5-KD cells reconstituted with pLNCX2 (empty vector) and moPrP^{WT} after no infection (NI) and infection with RML, ME7, MRC2 and 22L prions. (C). SCA data for independently isolated bulk cultures of CAD5-KD cells reconstituted with moPrP^{WT} and the indicated moPrP mutants following infection with ME7, MRC2 and 22L prion infected BHs respectively. Cultures A and B are the same bulk culture but at different serial passages. Data are shown as mean ± SD, ****P < 0.0001, ***P < 0.001, **P < 0.01, *P < 0.05 for cultures where number of infected cells was reduced in comparsion to cells reconstituted with moPrP^{WT}. Statistical analyses were performed using an unpaired 2-tailed t-test in GraphPad Prism 7.0 to CAD5-KD cells reconstituted with moPrP^{WT} bulk culture 1B. (D and E). SCA data after infection of CAD5 and bulk cultures of reconstituted CAD5-KD cells following infection with RML, ME7, MRC and 22L prion infected BHs. Data are shown as mean ± SD, ****P < 0.0001, ***P < 0.001, **P < 0.01, *P < 0.05 for cultures where number of infected cells was reduced in comparsion to cells reconstituted with moPrP^{WT}. Statistical analyses were performed using an unpaired 2-tailed t-test in GraphPad Prism 7.0 to CAD5-KD cells reconstituted with moPrP^{WT}.

glycosylated in the parental CAD5 cells. This was consistent with previous studies documenting that although PrP^{C} is necessary for replicating infectivity,[51] the actual level of expression is not important. Enari *et al* found that N2a/Bos2 cells, a clone of prion-susceptible cells, expressed PrP^{C} at the same low level as the parental N2a cells, whereas a resistant cell line expressed it at a 10 times higher level.[52] Moreover, over-expression of PrP did not increase susceptibility either, indicating

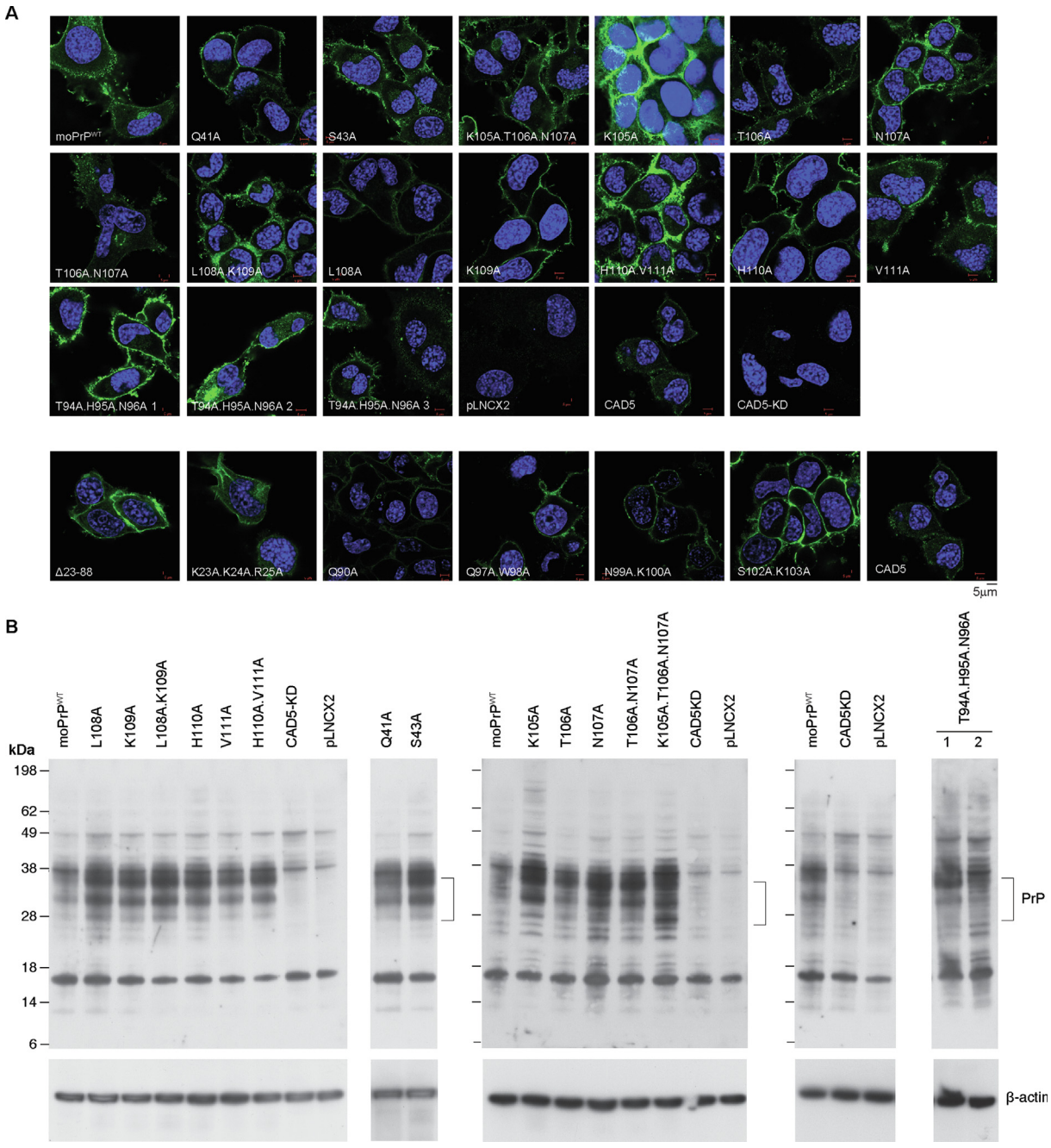

Figure 6. Analysis of PrP expression in reconstituted CAD5-KD cells. (A). Laser-scanning microscopy images of bulk cultures of CAD5, CAD5-KD and CAD5-KD cells after reconstitution with the indicated moPrP mutants. The analysis was carried out in two batches as indicated. DAPI, nuclear stain; mouse PrP, green. (B). Western blot analysis of PrP expression in bulk cultures of CAD5, CAD5-KD and CAD5-KD cells reconstituted with the indicated mutants.

that expression is a prerequisite for prion propagation, but other factors are also essential.[52] In accordance with this, Sandberg *et al* have found that propagation of RML in mice is not rate limited by PrP^C levels.[53]

Taken together, our data showed that amino acids 105.KTN.107, L108 and V111 within CC2 domain were required for propagation of RML, ME7, 22L and MRC2 prion strains. Other N-terminal residues either had no effect or only affected propagation of select strains. Q41A severely affected RML propagation in reconstituted PK1-KD cells but had no effect in CAD5-KD cells. Overall, the profile of N-terminal residues required for propagation of ME7 and RML were similar, whereas those required for 22L

were very different from these two strains and MRC2 shared features with all three.

Discussion

This study combined the development of mouse PK1-KD and CAD5-KD cell lines in which PrP^C has been stably silenced, with a systematic alanine replacement mutagenesis of the N-terminal 23–111 region of mouse *Prnp* to identify residues that are required for highly efficient prion propagation. We found that mutation of leucine 108 and valine 111 alone or simultaneous mutation of lysine 105, threonine 106 and asparagine 107, severely impacts propagation of RML, ME7, 22L and MRC2 mouse prion strains. Mutation of other N-terminal residues including the octapeptide repeats and CC1 domain either had no effect or only affected propagation of select prion strains. Replacements in the CC2 domain including aa105-111 dominantly inhibited prion propagation in the presence of endogenous PrP^C whilst other changes were not inhibitory. None of the mutants including aa105-111 blocked prion propagation when expressed in chronically RML prion-infected cells. Together, these results indicate that efficient prion propagation is dependent upon leucine 108 and valine 111 individually or lysine 105, threonine 106 and asparagine 107 together, acting at the infection stage.

N-terminal PrP residues 23–31 comprising the polybasic CC1 domain have been implicated in endocytosis via clathrin-coated pits[23,54–55], neurotoxicity[56–57], prion conversion[24,56] as well as association with amyloid- β oligomers.[29,31] Our results showed that for RML propagation, the critical residues within the CC1 domain were K23.K24.R25 and simultaneous replacement of all three residues was required to reduce the susceptibility to infection (Figure 3(C)), but this was reversed by the presence of wild-type PrP (Figure 4(A)).

Mutation of Q41 exhibited reduced RML propagation in PK1 cells, whereas none of the neighbouring residue replacements, namely SRY (36–38) and S43 had an effect (Figure 3(B&D)). There is no previous evidence implicating Q41 as a site for modulating prion propagation, or indeed for any other prion function. Of the alanine-mutants generated within aa23-88, 14 were within the OPR, each of which propagated RML at levels $\geq$ $moPrP^{WT}$ (Figure 3(B&C)) suggesting that the OPR domain does not play a critical role in regulating RML propagation. Another possible interpretation of our finding that no single OPR mutation affected propagation may be that our alanine mutagenesis strategy replaced histidines individually rather than replacing all simultaneously. Previous studies have suggested that the OPRs play only a limited role in disease pathogenesis[26] but supernumerary insertions of between one and nine additional OPRs, increase the risk of developing disease, with most cases showing an earlier onset.[25] Deletion of residues 23–88 abrogated RML propagation (Figure 2(C)) yet only mutations at KKR (23–25) and Q41 within this region were found to be inhibitory (Figure 3 (B)). When these two mutations were combined to determine any synergistic effects, none were observed; the results were an average of the individual mutations rather than additive (Figure 3(D)), indicating that KKR (23–25) and Q41 modulate the same pathway probably at an early stage of infection, rather than at a later stage once infection has been established (Figure 4(B)).

Minimal alanine substitutions (up to three residues) in the CC2 (90–111) region produced mutants that were well expressed in both PK1-KD and CAD5-KD cells (Figure 3(E) and 6). Q90A defined the most N-terminal position of the protein that showed a tenfold reduction in RML propagation (Figure 3(B)). Mutations at the C-terminal end of CC2 (H110A.V111A) also completely eliminated prion propagation. The CC2 domain mutants also reduced RML propagation when expressed in the presence of endogenous PrP^C in PK1 cells, a characteristic of competitive inhibition, whereas KKR (23–25) and Δ23-88 mutations were unable to act as competitive inhibitors (Figure 4(A)).

The next phase of this study was to examine if the requirement for KKR (23–25), Q41 and CC2 was RML-specific or a general requirement for prion infection and propagation. The results showed that Δ23-88 inhibited propagation of ME7 and MRC2 but 22L was still able to propagate albeit at a slightly lower efficiency, as in Uchiyama *et al*, who found that reconstitution with mouse PrP Δ23-88 restored susceptibility to 22L but not RML prions in $Prnp^{0/0}$ mice.[58] Similarly, aa23-25 (KKR) were required for propagation of ME7 and probably MRC2 prions but did not affect propagation of 22L prions. Khalifé *et al* found that deletion of aa23-26 (KKRP) in transgenic mice overexpressing ovine PrP resulted in variable susceptibility to prion infection, depending on the prion strain,[59] further highlighting aa23-25 as a strain-dependent modulator of prion propagation.

Like for RML in PK1 cells, all CC2 domain mutants affected propagation of ME7 prions. Mutations within aa94-98 and 105–111 inhibited 22L propagation whereas mutation of Q90, N99. K100 and S102.K103 had no effect. Propagation of MRC2 was inhibited by mutation of Q90 and aa105-111 whereas mutations within aa94-103 had no effect. Taken together these findings indicated that aa105-111 were required for efficient propagation, independent of the prion strain (RML, 22L, ME7 and MRC2).

Analysis of single alanine replacements within aa105-111 showed that L108A and V111A alone were as effective as L108A.K109A and H110A.

V111A for inhibiting prion propagation except L108A.K109A was more inhibitory for MRC2 than L108A. Neither L108 nor V111 are conserved between mice, hamsters and humans and are part of the epitope for the 3F4 antibody that can distinguish hamster and human PrP^C from mouse PrP^C. PK1-KD cells reconstituted with moPrP tagged with the 3F4 epitope do not support propagation of RML prions (Figure S8). Groveman *et al* have previously shown that substitution of the highly conserved CLC of four lysines (K100, K103, K105 and K109) with alanine or asparagine enhanced the formation of more pathogenic synthetic aggregates upon prion-templated seeding.[35] In accordance with this, we have found that K109A enhanced propagation of all four strains whereas K105A enhanced propagation of 22L, had no effect on RML and MRC2 but severely impeded propagation of ME7, contrary to replacement of charged residues enhancing formation of pathogenic aggregates. The four prion strains can be distinguished from each other by the N-terminal amino acids that are required for their efficient propagation: Mutants K105A and N107A cannot propagate ME7 but do not affect RML, MRC2 and 22L propagation; Δ23-88 and Q90A can propagate 22L but not RML, ME7 and MRC2; T106A can propagate RML but not ME7, MRC2 and 22L; and T94A. H95A.N96A and Q97A.W98A propagate MRC2 but not RML, ME7 and 22L (Figure7). RML and ME7 are the most similar, whereas 22L exhibits the greatest differences to RML and ME7 and MRC2 shares features with the other three.

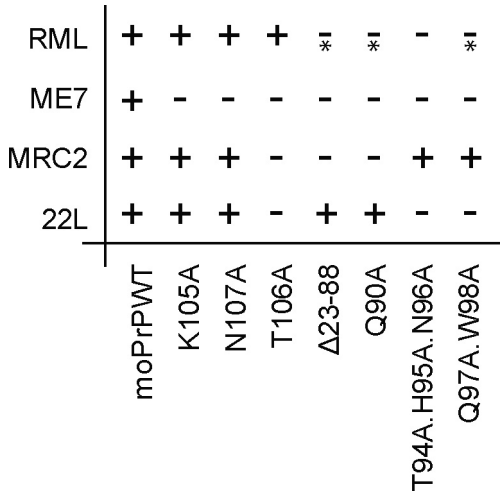

Figure 7. Selective propagation of mouse prion strains by N-terminal mutants of PrP. The ability of CAD-KD cells reconstituted with $moPrP^{WT}$ and the indicated mutants to propagate RML, ME7, MRC2 and 22L prions is shown. '+' designates support propagation whereas '–' an inability to support propagation. '*' indicates mutants that have only been tested for their ability to propagate RML upon reconstitution of PK1-KD cells.

The recent structures of mouse brain-derived wild-type RML and ME7 prion fibrils[69] show that a large portion (aa94-111) of the CC2 domain, which is disordered in PrP^C, becomes ordered in these prion fibrils (together with the LCR region), forming the first two β-strands in β-sheet-rich assemblies from both strains (Figure 8). The same is true for the GPI-anchorless variants of RML (aRML)[38] and 22L (a22L).[37] PrP residues that we identified as key for propagation of all four mouse prion strains (105.KTN.107, L108 and V111), are all located around the second β-strand. The two key hydrophobic residues (L108 and V111) and the aliphatic portion of T106 are part of a large hydrophobic cluster 1 (T106, L108, V111, I138, F140) that stabilises the PrP fold in each fibril (Figure 8). K105 contributes to the major basic patch on the surface of each fibril, which is thought to be an interaction hub for disease-associated PrP, as identified using motif grafted antibodies.[34,60] L108 is also one of the two amino acids (L108 and T189) that define the *Prnp*^{a} allele associated with a short incubation time upon prion infection in a range of inbred mouse strains.[61] Taken together, our data suggest that amino acid side chains that favour longitudinal cross-β stacking, coupled with strong lateral hydrophobic interaction via side chains of hydrophobic cluster 1 (Figure 8) are required for the specific ordering of the CC2 region.

Distinct prion strains present various degrees of sensitivity to mutations in this critical CC2 region. For example, single K105A or T106A or N107A mutations are sufficient to abrogate propagation of ME7, while having no effect on the propagation of RML (Figure 5E and Figure7). The atomic structures of ME7 and RML fibrils reveal structural differences between these strains, which include distinct interactions between T106 and neighbouring residues of hydrophobic cluster 1 (Figure 8(B)). Only three simultaneous alanine replacements in the 105.KTN.107 segment abrogate propagation of all mouse prion strains tested. The structure of the MRC2 strain is not yet known. Our data suggests that its ordering of the CC2 region will be similar overall, but with subtle differences that translate to the differential sensitivity to alanine replacements. Future experiments will aim to determine if 105.KTN.107 is sufficient for binding disease-associated PrP to initiate seeded protein polymerization or if another (co) factor is required for prion propagation.

Materials and Methods

Construction of plasmid DNAs

pBluescript SK + plasmid vector containing the full length ORF for mouse PrP was used as the template DNA. All residues within aa23-110 except glycine and proline were mutated to alanine in blocks of one, two or three amino acids, using the Stratagene QuikChange® site-directed

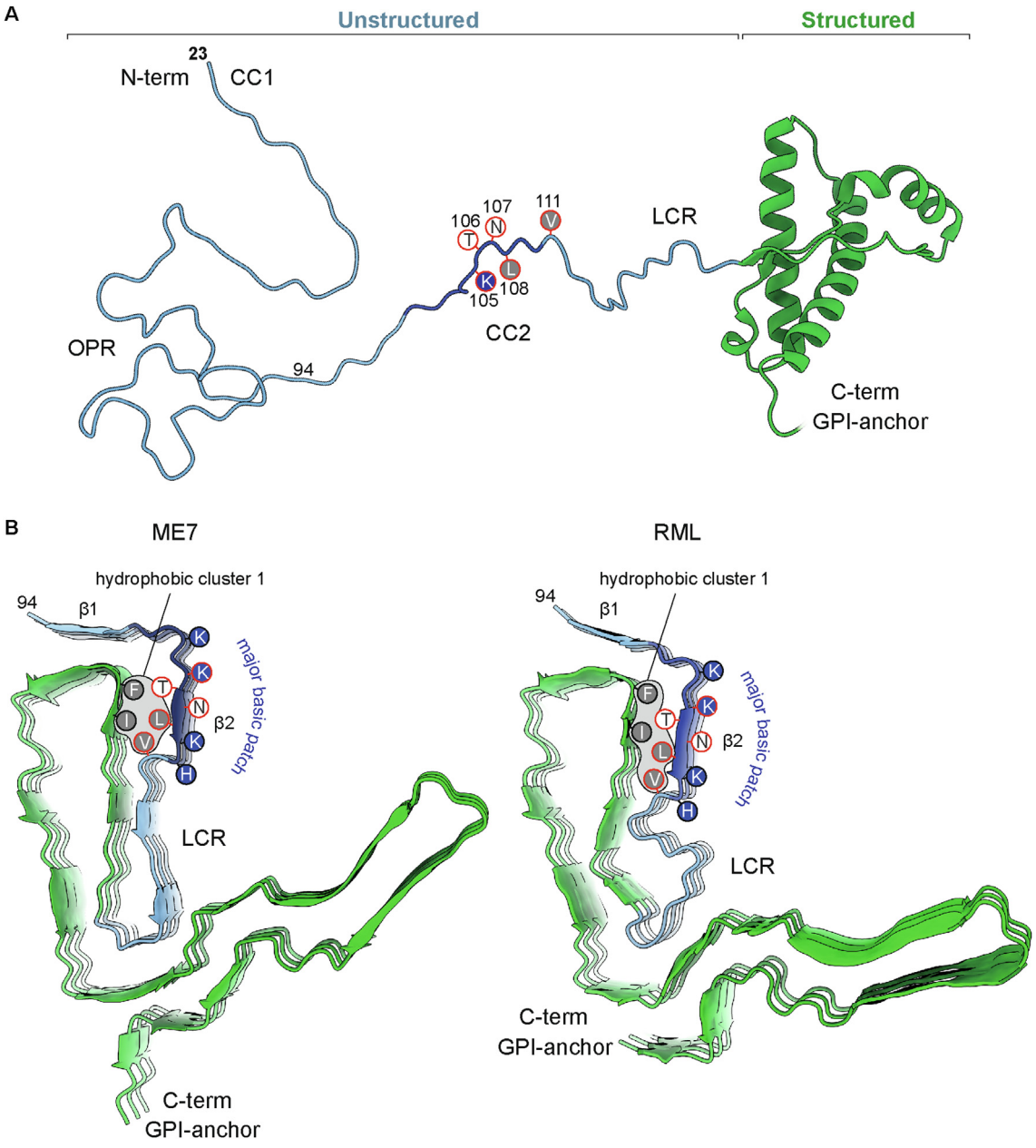

Figure 8. Mapping residues critical for prion propagation on PrP and prion fibril structures (A). Ribbon model of mature mouse PrP^C (residues 23–230, excluding post-translational modifications) built in UCSF Chimera[63] using an X-ray structure of $moPrP^C$ (pdb ID: 4H88)[64]. Positions of amino acid side chains found to be critical for prion propagation (basic, navy blue; neutral, white; hydrophobic, grey) are indicated. CC1, Charge Cluster 1; OPR, Octapeptide Repeats; CC2, Charge Cluster 2; LCR, Low-Complexity Region; GPI, glycosylphosphatidylinositol. (B). Mouse prion fibril structures from RML (pdb ID: 7QIG)[6] and ME7 (pdb ID: 8A00)[9] strains (3 subunits, ribbon representation, coloured as in (A)). Amino acid side chains found to be critical for prion propagation (marked with red circles) in the context of surrounding residues, coloured as in (A) are indicated. Major internal hydrophobic cluster 1 that contributes to PrP fold stability is indicated together with the major basic patch (navy blue). β-strands 1 and 2 are labelled.

mutagenesis system (Agilent Technologies, Santa Clara CA9051, USA). Mutations to alanine were designed using the moPrP protein sequence (UniProtKB entry P04925 NCBI Reference Sequence NM_011170.3). Codon GCC was selected for alanine replacement based on codon bias in the mouse genome. Positions at which native residues were proline or glycine were not targeted for mutagenesis. Sequence-verified mutated ORFs were inserted into the pLNCX2

retroviral vector (Clontech Takara, Mountain View CA 94043, USA). The siRNA target sequences were used to generate 64mer DNA oligonucleotides in accordance with the Oligoengine template design (https://www.oligoengine.com). The oligonucleotide pairs were annealed and inserted into the pRetroSuper silencing vector.

Retroviral expression

pRetrosuper shRNA and pLNCX2 constructs were packaged as ecotropic retroviruses in Phoenix ecotropic cells (ATCC, LGC Standards, Middlesex, UK) and used to stably transduce PK1 and CAD5 cells and derivatives thereof. The efficiency of stable transduction of CAD5-KD cells was increased by pseudotyping the ecotropic retroviruses using the vesicular stomatitis virus G (VSV-G) protein. Stable transduction of cells with pLNCX2 retroviruses was selected using 300 μg/ml G418 for PK1 and 400 μg/ml for CAD5 cells respectively. Stable silencing of endogenous PrP was achieved through stable expression of pRetrosuper shRNA constructs by selecting for puromycin resistance at 4 μg/ml for PK1 and 2 μg/ml for CAD5 cells respectively.

Scrapie cell assay

SCA was carried out as previously described.[49] Cells were plated at 18,000 cells/well of a 96-well plate, infected with prion infected brain homogenates the following day and grown for three weeks with 1:8 biweekly splits. At splits 4, 5 and 6, cell suspensions equivalent to 25,000 PK1 or 18,000 CAD5 cells were plated onto activated ELISPOT plates and probed for PK-resistant PrP using anti-PrP ICSM18 antibody ((1:6,000 of 1 mg/ml; D-Gen Ltd, UK) and goat anti-mouse anti-IgG1-AP secondary antibody (1:10,000 of 1 mg/ml; Southern Biotech).

Cells positive for PK-resistant PrP were quantified initially using WellScan software (Imaging Associates, Oxfordshire, UK) and more recently a Bioreader 7000F Alpha (BIOSYS GmbH, Germany).

Western blotting

PK1 cell lysates were prepared from frozen pellets by resuspending in 150 mM NaCl, 50 mM TrisHCl pH 7.5, 0.5% Triton-X-100, 0.5% sodium deoxycholate, 1 mM EDTA and 40U/ml benzonase. 25 μg of protein was fractionated on 16% Novex® Tris-Glycine mini gels, transferred to PVDF membrane and probed using anti-PrP ICSM18 antibody (D-Gen Ltd, London, UK).

CAD5 cell lysates were prepared from frozen cell pellets enriching for membrane bound proteins. Pellets were resuspended in 10 mM phosphate buffer (P5244, SigmaAldrich), incubated on ice at 4 °C for 5 mins followed by centrifugation at 15,000g for 15 mins. The pellet comprising the membrane fraction was resuspended in D-PBS and treated with benzonase (1–2 μl, 25KU equivalent to > 250units/μl) at room temperature for 15 mins. An equal volume of 2x sample buffer (125 mM TrisHCl pH6.8, 20% v/v glycerol, 4% w/v SDS, 4% v/v 2-mercaptoethanol, 8 mM 4-(2-aminoethyl)-benzene sulfonyl fluoride and 0.02% w/v bromophenol blue) was added and the samples boiled for 10 mins, followed by centrifugation at 15000g for 1 min. Supernatant was removed and protein concentration determined by the Bradford Assay.

15–25 μg of protein was fractionated on 12% BisTris NUPAGE gel (NP0341, ThermoScientific), transferred to PVDF and probed overnight at room temperature using anti-PrP ICSM35 antibody (0.2 μg/ml, D-Gen Ltd, London, UK). Antigen-antibody complexes were identified using goat anti-mouse AP (1:10,000 dilution of A2179, Sigma-Aldrich) and CDP-*Star*™ Substrate (T2146, ThermoScientific).

Immunofluorescence analysis

20,000 PK1 cells and derivatives thereof were seeded on sterile poly-L-lysine coated coverslips, grown at 37 °C and fixed using 4% w/v paraformaldehyde. Cells were permeabilised using 0.05% TritonX100. PrP expression was determined using the anti-PrP ICSM18 antibody (1:7,000 of 1 mg/ml) and visualised using AlexaFluor 488-conjugated goat anti-mouse secondary antibody.

50,000 CAD5 cells or derivatives thereof were seeded in each well of a chamber slide and grown at 37 °C for 3 days before fixation in 3.7% w/v paraformaldehyde. Anti-PrP ICSM18 (1 μg/ml) diluted in D-PBS containing 25% w/v superblock and 10% v/v penicillin streptomycin was added to each well of the chamber slide and incubated overnight at 4 °C. After extensive washing, the chamber slides were incubated again overnight at 4 °C with AlexaFluor 488-conjugated anti-mouse IgG (H + L) (115–545-116, Stratech Scientific ltd) in D-PBS containing 25% w/v superblock and 10% v/v penicillin streptomycin and DAPI (4′, 6-diamidino-2-phenylindole). After thorough washing, the chamber slides were imaged using a Zeiss LSM710 laser-scanning microscope, equipped with a 63x objective (Carl Zeiss, Cambridge, UK).

Cell viability assay and dot blot for moPrP expression

Cells were seeded at 2.5×10^4 cells/well in flat-bottomed 96-well plates, cultured for 3 days and lysed with CellTiter-Glo® reagent according to the manufacturer's instructions (Promega Corporation, Madison, WI 53711, USA). Plates were set to

shake for 2 mins and incubated for 10 mins at room temperature prior to recording luminescence (integration time = 100 ms).

For dot blot analysis, cells were harvested, counted and centrifuged at 300g for 4 mins. Cell pellet was resuspended in lysis buffer [50 mM TrisHCl pH 7.4, 150 mM NaCl, 0.5% Sodium deoxycholate and 0.5% Triton X-100]. Lysates were transferred to activated nitrocellulose using a dot blot manifold, at serial two fold dilutions of cells. PrP levels were determined using anti-PrP ICSM18 primary (1:4000 dilution of 1 mg/ml) and goat anti-mouse IRDye® 800CW infrared dye secondary antibody (1:4000 dilution) and quantified using an Odyssey infrared scanner.

RT-PCR analysis of Prnp gene expression in CAD5 cells

10,000 cells were lysed using the Taqman® Gene Expression Cells to CT™ kit (Ambion, Life Technologies) and the RNA reverse transcribed according to manufacturer's protocol. The resulting cDNA was assayed using Fam-labelled Prnp Taqman® assay (Mm00448389_m1, ThermoFisher) duplexed with VIC-labelled GAPDH endogenous control (Mm00712869_m1, ThermoFisher). Reactions were carried out in triplicate using an Applied Biosystems 7500 Fast Real-Time PCR machine with cycling conditions: 94 °C 15mins; 95 °C 15 s, 60 °C 60 s for 40 cycles.

CRediT authorship contribution statement

Savroop Bhamra: Conceptualization, Methodology, Data curation, Writing – original draft, Writing – review & editing. **Parineeta Arora:** Methodology, Data curation, Validation. **Szymon W. Manka:** Visualization, Writing – review & editing. **Christian Schmidt:** Methodology. **Craig Brown:** Methodology. **Melissa L. D. Rayner:** Methodology. **Peter-Christian Klöhn:** Supervision, Writing – review & editing. **Anthony R. Clarke:** Conceptualization, Supervision. **John Collinge:** Conceptualization, Supervision, Funding acquisition, Writing – review & editing, Project Administration. **Parmjit S. Jat:** Conceptualization, Methodology, Writing – original draft, Writing – review & editing, Supervision, Funding acquisition, Project Administration.

Declarations of interest

J. C. is a Director and shareholder of D-Gen Limited, an academic spin-out company working in the field of prion disease diagnosis, decontamination and therapeutics. D-Gen Ltd supplies PK1 cells, PK1-KD cells and the anti-PrP ICSM18 and ICSM35 antibodies used in this study. Other authors declare no conflicts of interest.

Acknowledgements

We are indebted to Emma Quarterman and Gigi Yang for providing cultures of CAD5 silenced cells that had been negatively sorted for cell surface PrP^C expression, Mitali Patel for undertaking the experiment presented in Figure S8 and Jonathan Wadsworth for helping us to develop the hypotonic lysis protocol for extracting membrane-associated proteins. We thank Ray Young and Richard Newton for graphics. Work was funded by the UKRI Medical Research Council.

Appendix A. Supplementary Data

Supplementary data to this article can be found online at https://doi.org/10.1016/j.jmb.2022.167925.

Received 16 August 2022;
Accepted 13 December 2022;
Available online 16 December 2022

Keywords:
alanine site-directed mutagenesis;
prion protein;
prion propagation;
prion strains;
scrapie cell assay

† S. B. and P. A. contributed equally to this work.
‡ Deceased.

References

1. Prusiner, S.B., (1998). Prions. *PNAS* **95**, 13363–13383.
2. Collinge, J., Clarke, A., (2007). A general model of prion strains and their pathogenicity. *Science* **318**, 930–936.
3. Collinge, J., (2016). Mammalian prions and their wider relevance in neurodegenerative diseases. *Nature* **539**, 217–226.
4. Terry, C., Wadsworth, J.D.F., (2019). Recent Advances in Understanding Mammalian Prion Structure: A Mini Review. *Front. Mol. Neurosci.* **12**, 169.
5. Kraus, A., Hoyt, F., Schwartz, C.L., Hansen, B., Artikis, E., Hughson, A.G., et al., (2021). High-resolution structure and strain comparison of infectious mammalian prions. *Mol. Cell* **81**, 4540–4551.
6. Manka, S.W., Zhang, W., Wenborn, A., Betts, J., Joiner, S., Saibil, H.R., et al., (2022). 2.7 Å cryo-EM structure of ex vivo RML prion fibrils. Nature. *Communications* **13**, 4004.
7. Terry, C., Wenborn, A., Gros, N., Sells, J., Joiner, S., Hosszu, L.L., et al., (2016). Ex vivo mammalian prions are formed of paired double helical prion protein fibrils. *Open Biol.*, 6.
8. Terry, C., Harniman, R.L., Sells, J., Wenborn, A., Joiner, S., Saibil, H.R., et al., (2019). Structural features distinguishing infectious ex vivo mammalian prions from non-infectious fibrillar assemblies generated in vitro. *Sci. Rep.* **9**, 376.

9. Manka, S.W., Wenborn, A., Betts, J., Joiner, S., Saibil, H. R., Collinge, J., et al., (2022). A structural basis for prion strain diversity. *bioRxiv.* 2022.05.17.492259.
10. Linden, R., Martins, V.R., Prado, M.A., Cammarota, M., Izquierdo, I., Brentani, R.R., (2008). Physiology of the prion protein. *Physiol. Rev.* **88**, 673–728.
11. Linden, R., Cordeiro, Y., Lima, L.M., (2012). Allosteric function and dysfunction of the prion protein. *Cell. Mol. Life Sci.* **69**, 1105–1124.
12. Linden, R., (2017). The Biological Function of the Prion Protein: A Cell Surface Scaffold of Signaling Modules. *Front. Mol. Neurosci.* **10**, 77.
13. Goold, R., Rabbanian, S., Sutton, L., Andre, R., Arora, P., Moonga, J., et al., (2011). Rapid cell-surface prion protein conversion revealed using a novel cell system. *Nat. Commun.* **2**, 281.
14. Rouvinski, A., Karniely, S., Kounin, M., Moussa, S., Goldberg, M.D., Warburg, G., et al., (2014). Live imaging of prions reveals nascent PrPSc in cell-surface, raft-associated amyloid strings and webs. *J. Cell Biol.* **204**, 423–441.
15. Bueler, H., Fischer, M., Lang, Y., Bluethmann, H., Lipp, H.-P., DeArmond, S.J., et al., (1992). Normal development and behaviour of mice lacking the neuronal cell-surface PrP protein. *Nature* **356**, 577–582.
16. Büeler, H., Aguzzi, A., Sailer, A., Greiner, R.-A., Autenried, P., Aguet, M., Weissmann, C., (1993). Mice devoid of PrP are resistant to scrapie. *Cell* **73**, 1339–1347.
17. Sakaguchi, S., Katamine, S., Shigematsu, K., Nakatani, A., Moriuchi, R., Nishida, N., et al., (1995). Accumulation of proteinase K-resistant prion protein (PrP) is restricted by the expression level of normal PrP in mice inoculated with a mouse-adapted strain of the Creutzfeldt- Jakob disease agent. *J. Virol.* **69**, 7586–7592.
18. Fischer, M., Rulicke, T., Raeber, A., Sailer, A., Moser, M., Oesch, B., et al., (1996). Prion protein (PrP) with amino-proximal deletions restoring susceptibility of PrP knockout mice to scrapie. *EMBO J.* **15**, 1255–1264.
19. Flechsig, E., Shmerling, D., Hegyi, I., Raeber, A.J., Fischer, M., Cozzio, A., et al., (2000). Prion protein devoid of the octapeptide repeat region restores susceptibility to scrapie in PrP knockout mice. *Neuron* **27**, 399–408.
20. Weissmann, C., Flechsig, E., (2003). PrP knock-out and PrP transgenic mice in prion research. *Br. Med. Bull.* **66**, 43–60.
21. Supattapone, S., Muramoto, T., Legname, G., Mehlhorn, I., Cohen, F.E., DeArmond, S.J., et al., (2001). Identification of two prion protein regions that modify scrapie incubation time. *J. Virol.* **75**, 1408–1413.
22. Taylor, D.R., Watt, N.T., Perera, W.S., Hooper, N.M., (2005). Assigning functions to distinct regions of the N-terminus of the prion protein that are involved in its copper-stimulated, clathrin-dependent endocytosis. *J. Cell Sci.* **118**, 5141–5153.
23. Ostapchenko, V.G., Makarava, N., Savtchenko, R., Baskakov, I.V., (2008). The polybasic N-terminal region of the prion protein controls the physical properties of both the cellular and fibrillar forms of PrP. *J. Mol. Biol.383*, 1210–1224.
24. Turnbaugh, J.A., Unterberger, U., Saa, P., Massignan, T., Fluharty, B.R., Bowman, F.P., et al., (2012). The N-terminal, polybasic region of PrP(C) dictates the efficiency of prion propagation by binding to PrP(Sc). *J. Neurosci.* **32**, 8817–8830.
25. Stevens, D.J., Walter, E.D., Rodriguez, A., Draper, D., Davies, P., Brown, D.R., et al., (2009). Early onset prion disease from octarepeat expansion correlates with copper binding properties. *PLoS Pathog.* **5**, e1000390.
26. Yamaguchi, Y., Miyata, H., Uchiyama, K., Ootsuyama, A., Inubushi, S., Mori, T., et al., (2012). Biological and biochemical characterization of mice expressing prion protein devoid of the octapeptide repeat region after infection with prions. *PLoS One* **7**, e43540.
27. Jackson, G.S., Murray, I., Hosszu, L.L.P., Gibbs, N., Waltho, J.P., Clarke, A., et al., (2001). Location and properties of metal-binding sites on the human prion protein. *Proc. Nat. Acad. Sci. USA* **98**, 8531–8535.
28. Lauren, J., Gimbel, D.A., Nygaard, H.B., Gilbert, J.W., Strittmatter, S.M., (2009). Cellular prion protein mediates impairment of synaptic plasticity by amyloid-beta oligomers. *Nature* **457**, 1128–1132.
29. Chen, S., Yadav, S.P., Surewicz, W.K., (2010). Interaction between human prion protein and amyloid-beta (Abeta) oligomers: role OF N-terminal residues. *J. Biol. Chem.* **285**, 26377–26383.
30. Freir, D.B., Nicoll, A.J., Klyubin, I., Panico, S., Mc Donald, J.M., Risse, E., et al., (2011). Interaction between prion protein and toxic amyloid beta assemblies can be therapeutically targeted at multiple sites. *Nat. Commun.* **2**, 336.
31. Fluharty, B.R., Biasini, E., Stravalaci, M., Sclip, A., Diomede, L., Balducci, C., et al., (2013). An N-terminal fragment of the prion protein binds to amyloid-beta oligomers and inhibits their neurotoxicity in vivo. *J. Biol. Chem.* **288**, 7857–7866.
32. Rushworth, J.V., Griffiths, H.H., Watt, N.T., Hooper, N.M., (2013). Prion protein-mediated toxicity of amyloid-beta oligomers requires lipid rafts and the transmembrane LRP1. *J. Biol. Chem.* **288**, 8935–8951.
33. Warner, R.G., Hundt, C., Weiss, S., Turnbull, J.E., (2002). Identification of the heparan sulfate binding sites in the cellular prion protein. *J. Biol. Chem.* **277**, 18421–18430.
34. Abalos, G.C., Cruite, J.T., Bellon, A., Hemmers, S., Akagi, J., Mastrianni, J.A., et al., (2008). Identifying key components of the PrPC-PrPSc replicative interface. *J. Biol. Chem.* **283**, 34021–34028.
35. Groveman, B.R., Raymond, G.J., Campbell, K.J., Race, B., Raymond, L.D., Hughson, A.G., et al., (2017). Role of the central lysine cluster and scrapie templating in the transmissibility of synthetic prion protein aggregates. *PLoS Pathog.* **13**, e1006623.
36. Hallinan, G.I., Ozcan, K.A., Hoq, M.R., Cracco, L., Vago, F. S., Bharath, S.R., et al., (2022). Cryo-EM structures of prion protein filaments from Gerstmann-Straussler-Scheinker disease. *Acta Neuropathol.* **144**, 509–520.
37. Hoyt, F., Alam, P., Artikis, E., Schwartz, C.L., Hughson, A. G., Race, B., et al., (2022). Cryo-EM of prion strains from the same genotype of host identifies conformational determinants. *PLoS Pathog.* **18**, e1010947.
38. Hoyt, F., Standke, H.G., Artikis, E., Schwartz, C.L., Hansen, B., Li, K., et al., (2022). Cryo-EM structure of anchorless RML prion reveals variations in shared motifs between distinct strains. *Nat. Commun.* **13**, 4005.
39. Kraus, A., Raymond, G.J., Race, B., Campbell, K.J., Hughson, A.G., Anson, K.J., et al., (2017). PrP P102L

and nearby lysine mutations promote spontaneous in vitro formation of transmissible prions. *J. Virol.* **91**, e01276–17.
40. Rogers, M., Yehiely, F., Scott, M., Prusiner, S.B., (1993). Conversion of truncated and elongated prion proteins into the scrapie isoform in cultured cells. *Proc. Nat. Acad. Sci. USA* **90**, 3182–3186.
41. Priola, S.A., Caughey, B., Race, R.E., Chesebro, B., (1994). Heterologous PrP molecules interfere with accumulation of protease-resistant PrP in scrapie-infected murine neuroblastoma cells. *J. Virol.* **68**, 4873–4878.
42. Shirai, T., Saito, M., Kobayashi, A., Asano, M., Hizume, M., Ikeda, S., et al., (2014). Evaluating Prion Models Based on Comprehensive Mutation Data of Mouse PrP. *Structure* **22**, 560–571.
43. Supattapone, S., Bosque, P., Muramoto, T., Wille, H., Aagaard, C., Peretz, D., et al., (1999). Prion protein of 106 residues creates an artificial transmission barrier for prion replication in transgenic mice. *Cell* **96**, 869–878.
44. Lloyd, S.E., Linehan, J.M., Desbruslais, M., Joiner, S., Buckell, J., Brandner, S., Wadsworth, J.D., Collinge, J., (2004). Characterization of two distinct prion strains derived from bovine spongiform encephalopathy transmissions to inbred mice. *J. Gen. Virol.* **85**, 2471–2478.
45. Mahal, S.P., Baker, C.A., Demczyk, C.A., Smith, E.W., Julius, C., Weissmann, C., (2007). Prion strain discrimination in cell culture: The cell panel assay. *Proc. Natl. Acad. Sci. USA* **104**, 20908–20913.
46. Cunningham, B.C., Wells, J.A., (1989). High-resolution epitope mapping of hGH-receptor interactions by alanine-scanning mutagenesis. *Science* **244**, 1081–1085.
47. Fersht, A.R., Daggett, V., (2002). Protein folding and unfolding at atomic resolution. *Cell* **108**, 573–582.
48. Tang, Q., Fenton, A.W., (2017). Whole-protein alanine-scanning mutagenesis of allostery: A large percentage of a protein can contribute to mechanism. *Hum. Mutat.* **38**, 1132–1143.
49. Klohn, P., Stoltze, L., Flechsig, E., Enari, M., Weissmann, C., (2003). A quantitative, highly sensitive cell-based infectivity assay for mouse scrapie prions. *Proc. Nat. Acad. Sci. USA* **100**, 11666–11671.
50. Qi, Y., Wang, J.K., McMillian, M., Chikaraishi, D.M., (1997). Characterization of a CNS cell line, CAD, in which morphological differentiation is initiated by serum deprivation. *J. Neurosci.* **17**, 1217–1225.
51. McNally, K.L., Ward, A.E., Priola, S.A., (2009). Cells Expressing Anchorless Prion Protein are Resistant to Scrapie infection. *J. Virol.* **83**, 4469–4475.
52. Enari, M., Flechsig, E., Weissmann, C., (2001). Scrapie prion protein accumulation by scrapie-infected neuroblastoma cells abrogated by exposure to a prion protein antibody. *Proc. Nat. Acad. Sci. USA* **98**, 9295–9299.
53. Sandberg, M.K., Al Doujaily, H., Sharps, B., Clarke, A.R., Collinge, J., (2011). Prion propagation and toxicity in vivo occur in two distinct mechanistic phases. *Nature* **470**, 540–542.
54. Shyng, S.-L., Moulder, K.L., Lesko, A., Harris, D.A., (1995). The N-terminal domain of a glycolipid-anchored prion protein is essential for its endocytosis via clathrin-coated pits. *J. Biol. Chem.* **270**, 14793–14800.
55. Fehlinger, A., Wolf, H., Hossinger, A., Duernberger, Y., Pleschka, C., Riemschoss, K., et al., (2017). Prion strains depend on different endocytic routes for productive infection. *Sci. Rep.* **7**, 6923.
56. Hara, H., Sakaguchi, S., (2020). N-terminal regions of prion protein: functions and roles in prion diseases. *Int. J. Mol. Sci.* **21**, 6233.
57. Turnbaugh, J.A., Westergard, L., Unterberger, U., Biasini, E., Harris, D.A., (2011). The N-terminal, polybasic region is critical for prion protein neuroprotective activity. *PLoS One* **6**, e25675.
58. Uchiyama, K., Miyata, H., Yano, M., Yamaguchi, Y., Imamura, M., Muramatsu, N., et al., (2014). Mouse-Hamster Chimeric Prion Protein (PrP) Devoid of N-Terminal Residues 23–88 Restores Susceptibility to 22L Prions, but Not to RML Prions in PrP-Knockout Mice. *PLoS One* **9**, e109737.
59. Khalife, M., Reine, F., Paquet-Fifield, S., Castille, J., Herzog, L., Vilotte, M., et al., (2016). Mutated but Not Deleted Ovine PrP(C) N-Terminal Polybasic Region Strongly Interferes with Prion Propagation in Transgenic Mice. *J. Virol.* **90**, 1638–1646.
60. Solforosi, L., Bellon, A., Schaller, M., Cruite, J.T., Abalos, G.C., Williamson, R.A., (2007). Toward molecular dissection of PrPC-PrPSc interactions. *J. Biol. Chem.* **282**, 7465–7471.
61. Lloyd, S.E., Thompson, S.R., Beck, J.A., Linehan, J.M., Wadsworth, J.D., Brandner, S., Collinge, J., Fisher, E., (2004). Identification and characterization of a novel mouse prion gene allele. *Mamm. Genome* **15**, 383–389.
62. Yang, S.L., Zhang, L.Y., Zhang, S.F., Zhang, M.Y., Zhu, M., Dong, Q., et al., (2022). Clinical and prognostic features of Heidenhain variant of Creutzfeldt-Jakob disease: A retrospective case series study. *Eur. J. Neurol.* **29**, 2412–2419.
63. Pettersen, E.F., Goddard, T.D., Huang, C.C., Couch, G.S., Greenblatt, D.M., Meng, E.C., et al., (2004). UCSF Chimera–a visualization system for exploratory research and analysis. *J. Comput. Chem.* **25**, 1605–1612.
64. Sonati, T., Reimann, R.R., Falsig, J., Baral, P.K., O'Connor, T., Hornemann, S., et al., (2013). The toxicity of antiprion antibodies is mediated by the flexible tail of the prion protein. *Nature* **501**, 102–106.